Characteristics of a piecewise smooth area-preserving map

Jian Wang,[1,2] Xiao-Ling Ding,[2] Bambi Hu,[3,4] Bing-Hong Wang,[5,6] Jian-Shan Mao,[1,2] and Da-Ren He[5,1,2,3,*]
[1]*Institute of Plasma Physics, Chinese Academy of Sciences, P.O. Box 1126, Hefei 230031, China*
[2]*Complexity Science Center, Yangzhou University, Yangzhou 225002, China*
[3]*Department of Physics and the Centre for Nonlinear Studies, Hong Kong Baptist University, Hong Kong, China*
[4]*Department of Physics, University of Houston, Houston, Texas 77204-5506*
[5]*CCAST (World Laboratory), P.O. Box 8730, Beijing 100080, China*
[6]*Department of Modern Physics, University of Science and Technology of China, Hefei 230026, China*
(Received 2 January 2001; published 16 July 2001)

We are reporting a study carried out in a system concatenated by two area-preserving maps. The system can be viewed as a model of an electronic relaxation oscillator with over-voltage protection. We found that a border-collision bifurcation may interrupt a period-doubling bifurcation cascade, and that some special features, such as ''quasicoexisting periodic orbits crossing border'' as well as the transition between ''quasitransience'' and chaotic orbits, accompany the process. These features belong to the so-called ''quasidissipative'' properties. Here ''quasitransience'' denotes the behavior of iterations outside elliptic islands. They are ''attracted'' to the islands. As soon as it reaches the islands, the iteration follows the conservative regulations exactly. This induces a kind of escaping from strange sets. The scaling behavior of the escaping rate is obtained numerically.

DOI: 10.1103/PhysRevE.64.026202 PACS number(s): 05.45.−a

I. INTRODUCTION

Chaotic phenomena in nonintegrable systems have attracted much attention since the 17th century. However, physicists have concentrated on everywhere-smooth systems where the function and derivatives of mathematical models are everywhere continuous. Often ignored are the piecewise smooth mathematical models that can describe many practical systems; such systems display certain kinds of catastrophes, crises, or extreme events. These systems may include relaxation and impact oscillators, dripping faucets, models of nerve cells or cardiopathy, and many others [1–11]. Their dynamic behaviors are very different from those of everywhere-smooth systems. He and co-workers have studied some relaxation oscillators [5–10]. They extensively studied an electronic relaxation oscillator and presented a detailed description of the system in Ref. [9]. The interesting phenomena observed in the system included type V intermittency [9,10], a kind of crisis induced by piecewise smooth characteristics [7], a multiple Devil's staircase [8], and the so-called ''coexistence of attractors induced by mapping holes'' [5,6,9].

Although most of the practical chaotic systems are dissipative, the study on chaotic phenomena in conservative systems is also important in theoretical studies. There are many conservative mathematical models that describe practical systems such as quantum systems, the solar system, and so on. Therefore, it is important to study piecewise smooth conservative systems. To the authors' knowledge, there are only a few publications relating to this topic [12–16]. Of these, Hu *et al.* have reported a study on quantum chaos in a non-KAM system exemplified by a particle in an infinite potential well subject to a periodic kicking force. They found a kind of diffusion in a stochastic web structure with special scaling properties [16].

This paper discusses another characteristic behavior in piecewise smooth conservative systems. It is addressed as a ''quasidissipative property.'' Its main feature is that elliptic islands attract iterations from outside. The phenomenon and some related behaviors accompany a process where a border-collision bifurcation [17] interrupts a period-doubling cascade.

The article is arranged as follows. Section II introduces the system; Sec. III discusses the quasidissipative properties, Sec. IV discusses the interruption of a period-doubling cascade by a border-collision bifurcation. The last section contains a discussion and conclusion.

II. THE SYSTEM

A. The system and its mathematical model

The aforementioned electronic relaxation oscillator can be briefly described as follows: A capacitor in the circuit is repeatedly charged and discharged, operated by two electronic control switches. The voltage across the capacitor, V, varies exponentially between a sine-modulated upper threshold and a constant lower threshold. The upper threshold can be expressed as $U(t)=U_{max}-U_0\sin(\omega t)$ (U_{max} is a constant), and the lower one as $W(t)=U_{min}$ (constant). At time t_n, V decreases from an upper threshold value $V_n=U(t_n)$. It suddenly rises at t^* when reaching a lower threshold value $V^*=W(t^*)$. Then it suddenly drops again when reaching another upper threshold value V_{n+1} at time t_{n+1}. In this way V oscillates continuously. From the ordinary differential equations describing the circuit [9], one can deduce the Poincarè mapping as (see the Appendix also)

*Corresponding author. Department of Physics, Yangzhou University, Yangzhou 225002, China. Email address: drhe@mail.yzu.edu.cn

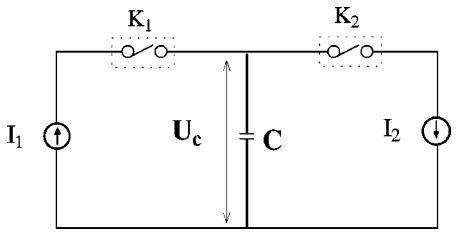

FIG. 1. A schematic drawing showing the circuit of the electronic relaxation oscillator, which can be described by maps (6) and (7).

$$x_{n+1}-B_2+A_2\ln[C_2+U_0(\sin 2\pi x_{n+1})] = x_n+A_1\ln[C_1/B_1+(U_0/B_1)\sin(2\pi x_n)] \pmod 1, \tag{1}$$

where x_n (n is an integer) is the normalized phase of the upper modulation signal corresponding to t_n, while A_i, B_i, C_i ($i=1,2$) are constants determined by the parameters of the circuit. Their expressions can be found in the Appendix.

Most of the practical relaxation oscillators are more complicated. Often a two-dimensional map is necessary for describing them. In Ref. [18] one may find an example. In order to simulate the cases we may reform map (1) by letting one parameter, such as the lower threshold, become a variable. In some practical cases, if V takes very large values in a phase region, over-voltage protection has to be considered. These two changes will make map (1) a two-dimensional piecewise smooth version.

A schematic drawing of the new circuit is shown in Fig. 1 (where $I_1 \gg I_2$), and the relaxation oscillation as well as both the thresholds are shown by Fig. 2. We suppose that for the capacitor, the charging current I_1 takes an infinitely large value, and the discharging current I_2 remains constant. To express the voltage protection we let the upper threshold equal a constant E in the phase region F where $V>E$. We feel it is more convenient to introduce a new parameter c,

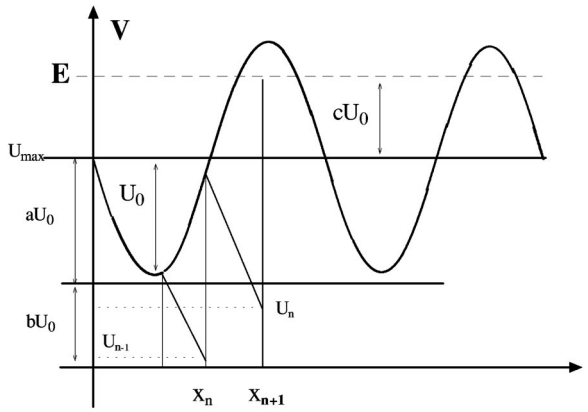

FIG. 2. A drawing showing the relaxation oscillation of the voltage across the capacitor and both the upper and lower thresholds, as well as the over-voltage protection.

which is defined as $c=E/U_0$, to describe the phenomenon as can be seen in Fig. 2. Now the form of the upper threshold can be expressed as

$$\begin{cases} U_n^{up}=U_{max}-U_0\sin(2\pi x_n), & x_n \notin F \\ U_n^{up}=U_{max}+cU_0, & x_n \in F, \end{cases} \tag{2}$$

where $F=(x_{F_1},x_{F_2})=[0.5+\arcsin(c)/2\pi, 1-\arcsin(c)/2\pi]$ is the phase region of over-voltage protection and the parameter c satisfies the condition $0<c<1$. As mentioned, the lower threshold is modulated by the underlying x_n phase according to a certain rule. We define another variable y_n as

$$\begin{cases} y_{n+1}=y_n-\dfrac{1}{b}\sin(2\pi x_n), & x_n \notin F \\ y_{n+1}=y_n+\dfrac{4\pi}{bU_0}x_n, & x_n \in F \end{cases} \tag{3}$$

and suppose that the lower threshold is a linear function of it,

$$U_{min}(y_n)=U_{max}-aU_0-by_nU_0. \tag{4}$$

The parameters satisfy $a>1$ and $b>0$. When $y_n=0$, one has $U_{min}=U_{max}-aU_0$, and when $y_n=1$, one has $U_{min}=U_{max}-aU_0-bU_0$. From the geometry shown in Fig. 2 one can easily understand that the lower threshold should be confined in the range $(U_{max}-aU_0, U_{\max}-aU_0-bU_0)$, and y_n should be confined in $[0,1]$. Also he can obtain

$$C[U(x_n)-U_{min}(y_n)]=I_2\frac{2\pi(x_{n+1}-x_n)}{\omega}, \tag{5}$$

where C is the capacitance of the charged capacitor and ω is the frequency of the modulating signal of the upper threshold as mentioned in Sec. II A. From Eqs. (2)–(5) and with the condition $C\omega/I_2=1$ as well as $bU_0/2\pi=1$, one can get the following map describing the current system,

$$x_{n+1}=f_{1x}=x_n+y_{n+1}+\frac{a}{b} \pmod 1, \tag{6}$$

$$y_{n+1}=f_{1y}=y_n-\frac{\sin 2\pi x_n}{b} \pmod 1$$

when $x_n \notin F$,

$$x_{n+1}=f_{2x}=x_n+y_n+\frac{a+c}{b} \pmod 1, \tag{7}$$

$$y_{n+1}=f_{2y}=y_n+2x_n \pmod 1$$

when $x_n \in F$. In the current study we take $a=2.0$, b and/or c are chosen as the control parameters.

B. Some properties of the system

1. Noninvertibility of the map

It is easy to verify that the absolute value of the determinant of the Jacobian matrix of maps (6) or (7) equals a unit.

That means either Eqs. (6) or (7) is a conservative mapping. The question is whether the nonsmooth concatenation map is still conservative. This question shall be answered later. Note that there is no resistor in the circuit. It is supposed that in such a case the current sources can work without supply or expense of energy. This can be approximately realized in an experiment by using some modern devices.

The backward maps of Eqs. (6) and (7) are

$$x_n = f_{1x}^{-1} = x_{n+1} - y_{n+1} - a/b,$$
$$y_n = f_{1y}^{-1} = y_{n+1} + \sin(2\pi x_n)/b, \tag{8}$$

when $x_n \notin F$,

$$x_n = f_{2x}^{-1} = -x_{n+1} + y_{n+1} + (a+c)/b,$$
$$y_n = f_{2y}^{-1} = y_{n+1} - 2x_n, \tag{9}$$

when $x_n \in F$. It tells us that either map (6) or (7) is invertible. However, due to the fact that the condition of selecting solutions in backward maps (8) and (9) is determined by x_n instead of x_{n+1}, one can still find two (x_n, y_n) values for each (x_{n+1}, y_{n+1}) according to either the function f_1 or f_2. That means the concatenation map is noninvertible. This behavior may be addressed as noninvertibility induced by the piecewise smooth property.

2. Some properties of the map without protection

If there is no voltage protection, map (7) does not appear. The remaining map (6) can be viewed as a kind of standard map [19]. The main characteristics of it have been discussed already in many references. We shall only briefly discuss the fixed points, the period-2 orbits, and the critical parameter value where the system is going to be globally chaotic, as well as the period-doubling bifurcation of a fixed point.

The fixed-point equation of map (6) can be expressed as

$$\frac{1}{b}\sin(2\pi x^*) = 0, \pm 1, \pm 2, \ldots,$$
$$y^* = -\frac{a}{b}, \tag{10}$$

when $x_n \notin F$. As is well known, their stability can be determined by

$$\mathrm{Tr}(J_{a6}) = 2 - \frac{2\pi}{b}\cos(2\pi x^*), \tag{11}$$

where J_{a6} is the Jacobian matrix of map (6) at the fixed point. When $|\mathrm{Tr}(J_a 6)| < 2$, it is an elliptic point; it becomes hyperbolic if $|\mathrm{Tr}(J_{a6})| > 2$. Therefore, taking $\sin(2\pi x^*) = 0$, one has a fixed point at $(x_1^*, y_1^*) = (0, -a/b)$. It is elliptic if $b > \pi/2$. Also, another fixed point located at $(x_2^*, y_2^*) = (0.5, -a/b)$. It is always hyperbolic.

There is another group of fixed points. When $0 < b < 1$, from $\sin(2\pi x^*) = \pm b$, one can get the following four fixed points:

$$x^* = \frac{\arcsin b}{2\pi}, \quad 0.5 - \frac{\arcsin b}{2\pi}, \quad 0.5 + \frac{\arcsin b}{2\pi},$$
$$1.0 - \frac{\arcsin b}{2\pi}; \tag{12}$$
$$y^* = -\frac{a}{b}.$$

Similarly, one can find that two of them, $(\arcsin b/2\pi, -a/b)$ and $(1 - \arcsin b/2\pi, -a/b)$, are elliptic when the condition $b \in (\pi/\sqrt{4+\pi^2}, 1)$ is satisfied. The other two points at $(0.5 - \arcsin b/2\pi, -a/b)$ and $(0.5 + \arcsin b/2\pi, -a/b)$ are always hyperbolic.

We can discuss a period-2 orbit in a similar way. The two periodic points (x_1, y_1) and (x_2, y_2) satisfy the following equations:

$$x_2 = x_1 + y_2 + \frac{a}{b} + m_1,$$
$$y_2 = y_1 - \frac{1}{b}\sin(2\pi x_1), \tag{13}$$

$$x_1 = x_2 + y_1 + \frac{a}{b} + m_2,$$
$$y_1 = y_2 - \frac{1}{b}\sin(2\pi x_2), \tag{14}$$

where m_1, m_2 are integers. From the equations one knows that there are two possible relationships between x_1 and x_2. They are

$$x_1 = -x_2$$

or

$$x_1 = 0.5 - x_2.$$

We shall only discuss the first case here. In this simple case the periodic points satisfy

$$4x_1 = \frac{1}{b}\sin(2\pi x_1) + m_2 - m_1,$$
$$x_2 = -x_1,$$
$$y_1 = 2x_1 - \frac{a}{b} - m_2, \tag{15}$$
$$y_2 = -2x_1 - \frac{a}{b} - m_1.$$

In the current study we shall only discuss the case $m_1 = m_2 = 0$. The stability condition of this orbit is $|\mathrm{Tr}(J_{a6} \circ J_{a6}| < 2$, i.e.,

$$0<\frac{2\pi}{b}\cos(2\pi x_1)<4. \tag{16}$$

So, the stable range of the orbit is $1<b<\pi/2$.

Shenker and Kadanoff [20] studied the typical standard map, which was expressed by

$$x_{n+1}=x_n+y_{n+1} \pmod 1, \tag{17}$$

$$y_{n+1}=y_n-\frac{K}{2\pi}\sin(2\pi x_n)(\mathrm{mod}\ 1).$$

They analytically proved that the last remaining KAM torus that stretches from $x=0$ to $x=1.0$ is going to be broken at a critical parameter value $K=K_c=0.971\,635\,4\ldots$. The system becomes globally chaotic when $K>K_c=0.971\,635\,4\ldots$. Referring to their work and the function forms of map (6), one can learn that in map (6) the last remaining KAM torus is going to be broken at $b=b_c=6.466\,84\ldots$. When $b<b_c$ the system is globally chaotic.

Now we can discuss the bifurcation of the fixed point $(x_1^*,y_1^*)=(0,-a/b)$. From the above discussion one knows that it is stable when $b>\pi/2=1.570\ldots$. It bifurcates at $b=\pi/2$ and produces a period-2 orbit. This period-2 orbit loses stability at $b=1$. When $b<1$, the system produces a period-4 orbit as well as the two elliptic fixed points expressed by Eqs. (12). This entire process happens beneath the threshold b_c, i.e., inside the globally chaotic region.

3. Some properties of the map with protection

Starting from an initial value near an elliptic point, the iterations draw a commensurate or incommensurate cycle. They are addressed as KAM cycles. According to famous KAM theorem, there is the largest KAM cycle, which is incommensurate and separates the periodic or quasiperiodic motion inside it and the chaotic motion outside it. Usually the part of phase space inside the largest KAM cycle is addressed as an elliptic island.

Referring to Sec. II A we denote the two borderlines between the definition ranges of maps (6) and (7) by $\{(x,y)|x=x_{F_1}\}$ and $\{(x,y)|x=x_{F_2}\}$. When voltage protection is applied they may hit some KAM cycles in an island and destroy them. Another new feature is the possibility of the appearance of ''periodic orbits crossing border.'' It is easy to realize that a periodic orbit of map (7) cannot show periodic points only in its own definition range. The points should cross the border. Such an orbit may be expressed as

$$\prod_{i=0}^{j} f_2^{q_i}f_1^{p_i}(D)=D, \tag{18}$$

where p_i,q_i,i, and j are integers, D denotes a point in the periodic orbit, and f_1 and f_2 are mapping functions listed in Eqs. (6) and (7). The criterion of the stability of the orbit is the same as mentioned before. In the current study we mainly discuss such orbits numerically due to the complicated form of the mapping function. Some analytical calculation has been made with a simplified model [21]. The system with voltage protection can show other interesting properties. Two of them will be discussed in the next two sections.

III. THE QUASIDISSIPATIVE PROPERTIES

There is a discontinuous set in the current system

$$\Gamma=\cup_{m=1}^{n_1}[f_j^{-(m-1)}(\{(x,y)|x=x_{F_i}\})] \quad (i=1,2;j=1,2), \tag{19}$$

which may play an important role. Here n_1 is the periodic number of the studied elliptic orbit, $j=1$ or 2 depending on which definition range the point on the considered backward image of the borderline (not the borderline itself) falls in. It should be noted that the backward images are almost always double due to the aforementioned noninvertibility, and that after the stretching and turning by a backward iteration, the points on following backward images of the borderlines will usually fall in the definition ranges of both maps (6) and (7). It is easy to see that any KAM cycle that collides with set Γ should dissolve. This set divides the phase plane into regions, which may be addressed as ''KAM regions.'' The KAM theorem now is correct only inside each KAM region. The iterations across KAM regions may not obey KAM theorem. For example, iterations from some initial points outside an elliptic island may cross some borders of KAM regions and go into the island (as will be shown below).

A. The quasidissipative properties

Now we discuss the case when the parameters are chosen as $a=2.0$, $b=0.933\,564<1$, $c\in[0.7,0.9]$. As mentioned [below Eq. (12)], if there is no voltage protection, two stable elliptic points are located at $e_{1*}=(0.191\,659,0.857\,671)$ and $e_{2*}=(0.808\,341,0.857\,671)$. There should be a period-4 elliptic orbit produced by the period-doubling bifurcation of the ordinary elliptic point (x_1^*,y_1^*). The corresponding period-1 hyperbolic points are located at $h_{1*}=(0.0,0.857\,671)$, $h_{2*}=(0.5,0.857\,671)$, $h_{3*}=(0.308\,341,0.857\,671)$, and $h_{4*}=(0.691\,659,0.857\,671)$.

In the current system (with protection) we address the elliptic island around the elliptic point e_{1*} as e_1 and the island around the point e_{2*} as e_2. At the parameter value $c=c_0=0.933\,564$, e_{2*} collides with $\{(x,y)|x=x_{F_2}\}$, the right boundary of region F. When c decreases further, e_{2*} falls into the protection region and vanishes. In the next section we shall show that the period-4 orbit also disappeared via a collision with a borderline. Only elliptic island e_1 remains. When $c=0.89$, we choose 500×500 initial values evenly in the range $x\in[0,1]$ and $y\in[0,1]$ and compute iterations of maps (6) and (7). The iterations do not obey KAM theorem since they are trapped into e_1 island as shown in Fig. 3. However, as soon as they enter the island, they perform the typical conservative behavior. Let us explain this behavior.

The noted noninvertibility induced by the piecewise smooth property produces double images for each point D in e_1 island as shown in Fig. 4. One of the backward images, $f_1^{-1}(D)$, is inside the island. Another one, $f_2^{-1}(D)$, is outside

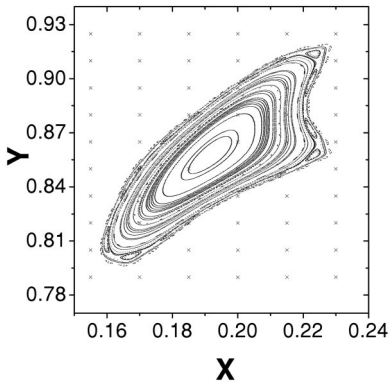

FIG. 3. The crosses show the chosen initial values. The first 10 000 iterations from these initial values were ignored to avoid the quasitransience, and the following 1000 iterations were recorded to obtain the dotted lines, which show elliptic island e_1. The parameter values were chosen as $a=2.0$, $b=0.933\,564$, and $c=0.89$.

the island and located inside the protection region. The first backward image leads to the iterations following conservation laws. The second backward image leads to behavior simulating transience in dissipative systems, since they cross a border of KAM regions. Therefore, the island may be called a quasi-attractor. The iterations outside the island may be addressed as quasitransience (QT). The set of the initial values, from which iterations tend to quasiattractors, may be called a quasibasin. This kind of dynamic behavior may be addressed as quasidissipativity. It seems that the concatenation map is neither dissipative nor conservative. It simulates a dissipative one out of some regions (the elliptic islands), but simulates a conservative one inside these regions. This phenomenon may be interesting and important in some cases, as will be discussed in the last section.

B. The quasigaps inside the quasitransient iterations

Figure 5 shows the QT recording from 500×500 initial

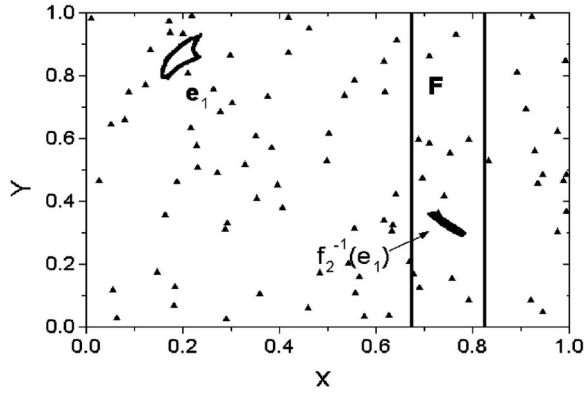

FIG. 4. For the computation, 500×500 initial values were chosen evenly on the phase plane. The small triangles show the initial values for which the iteration spent 2500 steps or more to reach e_1 island. The parameter values were chosen as $c=0.89$, $a=2.0$, and $b=0.933\,564$. The two vertical linear lines denote the borderlines, $\{(x,y)|x=x_{F_1}\}$ and $\{(x,y)|x=x_{F_2}\}$, of the voltage protection region F.

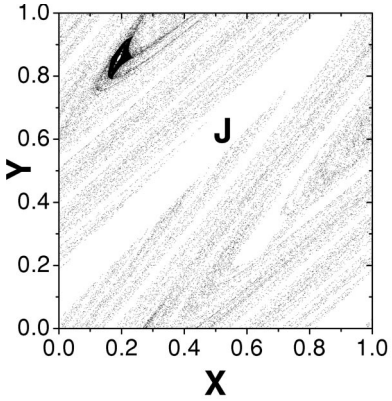

FIG. 5. The figure was drawn by recording 10 000 iterations from evenly chosen 500×500 initial values. The parameter values were chosen as $c=0.89$, $a=2.0$, and $b=0.933\,564$. The white region indicated by J was explained in the text.

points evenly chosen on the phase plane when $c=0.89$. One may note the strange pattern there formed by white regions. The pattern should indicate the regions where the visit of iterations is almost prohibited. We may denote the regions as ''quasigaps.'' The largest quasigap is the white band indicated by J in the figure. It becomes a gap because its backward images do not exit as shown by Fig. 6. As can be seen, $f_1^{-1}(J)$ falls in the definition region of f_2, while $f_2^{-1}(J)$ falls in the definition region of f_1. We found that the other white regions are mainly occupied by the first forward image of J as shown by the black regions in Fig. 7. These regions are well consistent with the curly quasigap regions shown in Fig. 5. Thus it is easy to understand that the visit to the region is almost prohibited. There may be some very small ''white'' regions occupied by further forward images of J but, obviously, they can be visited with more and more possibilities.

C. Escaping from a strange set induced by quasidissipative property

Here, we show that all the chaotic orbits in the chaotic sea outside e_1 island become QT. This can be viewed as a kind

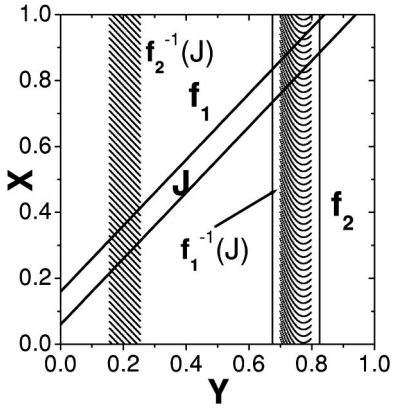

FIG. 6. The dotted regions show the backward images of the quasigap region J as indicated by the solid oblique lines. The two vertical solid lines indicate the borderlines, $\{(x,y)|x=x_{F_1}\}$ and $\{(x,y)|x=x_{F_2}\}$, of protection region F. The parameter values are $c=0.89$, $a=2.0$, and $b=0.933\,564$.

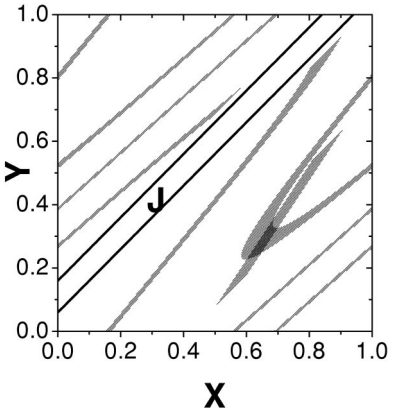

FIG. 7. The figure was computed with the parameter values $c=0.89$, $a=2.0$, and $b=0.933\,564$. The black regions show the first forward image of the quasigap region J. J is indicated by solid oblique lines.

of escaping from a strange set via a leaking hole [22]. The hole H can be defined as follows.

Let us denote the intersection of $f_2^{-1}(e_1)$ and F, the set of points inside the protection region (see Fig. 4), by I and the set of the quasigap J and its first forward image by G. The hole is then defined as the difference set between set I and the intersection of I and G, i.e.,

$$H=I\backslash(I\cap G),$$

$$I=F\cap f_2^{-1}(e_1),$$

$$F=\{(x,y)|x_{F1}<x<x_{F2}\}, \tag{20}$$

$$G=J\cup(f_j(J)),$$

where j equals 1 or 2 depending on which definition range the point of J falls in. Figure 8 shows a magnification of the part of phase space around the leaking hole when $c=0.89$. According to the definition of H, only the first image of J is shown in the figure.

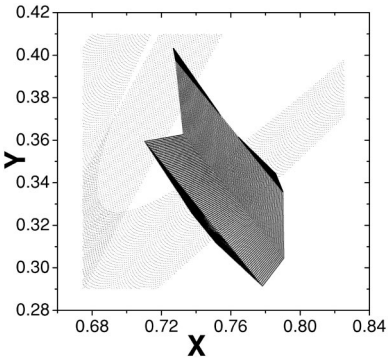

FIG. 8. A magnification of the part of phase space around the leaking hole. The black region shows the set I, the intersection between $f_2^{-1}(e_1)$, and F. The dotted regions show set G, the set of quasigap J, and its first image. The leaking hole H was defined as $H=I\backslash(I\cap G)$. The parameter values were chosen as $c=0.89$, $a=2.0$, and $b=0.933\,564$.

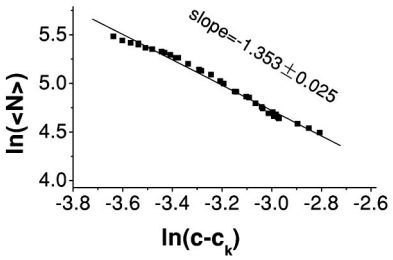

FIG. 9. Scaling behavior of mean transient time $\langle N\rangle$. The squares denote the computed data. The linear line was obtained by the least square fitting. The parameter values were chosen as $c_k=0.7419$, $a=2.0$, and $b=0.933\,564$.

In order to give a quantitative description of the escaping, we define the mean transient time $\langle N\rangle$ for the ensemble of initial points as follows:

$$\langle N\rangle=\lim_{n\to\infty}\frac{\sum_{i=1}^{n}N_i}{n}, \tag{21}$$

where n is the number of initial points of the ensemble and N_i is the length of QT from each initial point. The validity of the definition should rely on the fact that $\langle N\rangle$ tends to a constant when $n\to\infty$. To prove this in the underlying system, a numerical investigation has been made. The results certify that the definition is valid when set I, the intersection between $f_2^{-1}(e_1)$ and F, is not an empty set. Our computation also shows that the leaking hole size decreases and $\langle N\rangle$ increases as c is getting smaller obeying a power law $\langle N\rangle^{-1}\propto(c-c_k)^{\nu}$. This is also in agreement with the conclusion reported in Ref. [22]. The critical value $c_k=0.741\,90\pm0.000\,02$ indicates the vanishing point of set I. It is also the vanishing point of the leaking hole H. The good scaling behavior shown in Fig. 9 convinced us of the scaling property and the exponent $\nu=1.353\pm0.025$.

IV. PERIOD-DOUBLING BIFURCATION

For an investigation on period-doubling bifurcation, we choose the parameter values $a=2.0$ and $c=0.933\,564$. Parameter b serves as the driving parameter. In this situation the voltage protection region F becomes a fixed one, i.e., $F=(x_{F_1},x_{F_2})=(0.691\,659\,371\,92,0.808\,340\,628\,07)$.

As discussed in Sec. II, if there is no voltage protection, fixed point $(x_1^*,y_1^*)=(0,-a/b)$ is stable when $b>\pi/2$. It period doubles first at $b=\pi/2\simeq1.570$. The period-2 orbit loses stability at $b=1$. When $b<1$, the system produces a period-4 orbit as well as the four fixed points expressed by Eq. (12). This entire process happens below the threshold b_c, i.e., inside the globally chaotic region. The period-doubling bifurcation cascade will become complete. However the situation becomes very different in the underlying system as will be discussed in this section.

Figure 10(a) shows the phase plane after the first period-doubling bifurcation when $b=\pi/2.1\simeq1.495\,996\,5$. The original elliptic point, (x_1^*,y_1^*), now becomes hyperbolic at

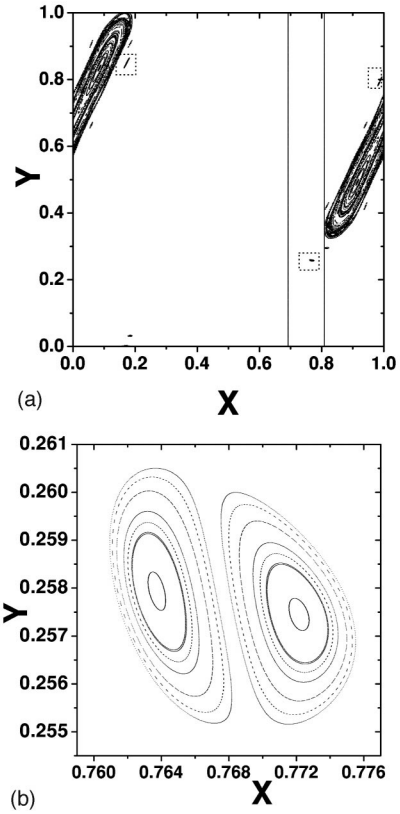

FIG. 10. (a) The phase plane after the first period-doubling bifurcation. The parameter values were selected as $b=\pi/2.1$, $a=2.0$, and $c=0.933\,564$. 20×20 evenly distributed initial values were chosen. The first 4×10^5 iterations from the initial values were ignored to avoid the quasitransience. Then the following 1000 iterations were recorded to obtain the elliptic islands as shown by dotted lines. A period-6 orbit that crosses the border is denoted by three dashed squares. The two solid vertical lines show the over-voltage protection region F. (b) A magnification of the part in (a) occupied by the dashed square inside region F.

(0.0,0.6631). The new period-2 elliptic points are located at (0.085 690 9,0.834 48) and (0.914 309,0.491 717). All the orbits inside the chaotic sea around their islands become QT, as discussed before. The ''periodic orbit crossing border'' is denoted by three squares in the figure. Figure 10(b) shows the magnification of the square inside region F, the over-voltage protection region. It tells us that the new orbit is a period-6 orbit and can be expressed as

$$f_2 f_{1l} f_{1r} f_2 f_{1l} f_{1r}(D)=D, \tag{22}$$

where D denotes any point inside the period-6 elliptic islands, and f_{1l} or f_{1r} denotes the mapping function (6) in its left or right half of the definition region, respectively. The criterion for the stability of the orbit is $|\mathrm{Tr}(J_a)<2|$ where $J_a=J_{a7}\circ J_{a6}\circ J_{a6}\circ J_{a7}\circ J_{a6}\circ J_{a6}$. This orbit is ''quasicoexisting'' with the period-2 orbit. Each of them has its quasibasin. Our numerical results show that this period-6 orbit exists only in a very small range $b\in(\pi/2.1-10^{-3},\pi/2.1+10^{-2})$.

When b becomes even smaller, the period-2 elliptic island moves toward borderline $\{(x,y)|x=x_{F_2}\}$. At $b\simeq1.37$ it becomes a tangent to the borderline. When $b\simeq1.324$, the escaping hole vanishes via a similar mechanism as discussed in the last section so that the QTs become chaotic orbits again. We can determine the similar scaling behavior for the mean transient time as in the last section. The obtained rule is $\langle N\rangle^{-1}\propto(b-b_k)^{\nu}$. Here the critical value $b_k=1.3245$ and the scaling exponent is $\nu\simeq1.39$.

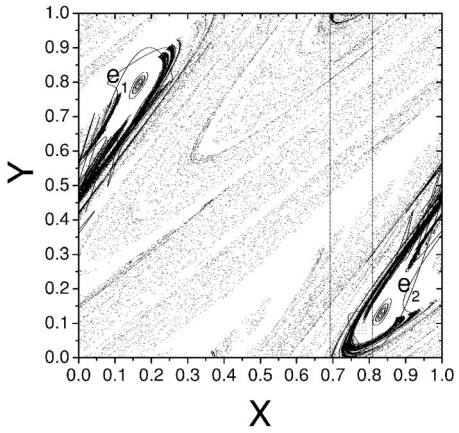

FIG. 11. The figure was computed with the parameter values $b=1.3$, $a=2.0$, and $c=0.933\,564$. 10×40 initial values were evenly chosen inside region F, which was indicated by two vertical solid lines. The following initial values inside the remaining elliptic islands were also taken: $(x,y)=(0.816\,211\,53,0.125\,46)$, $(0.821\,527\,4,0.126\,102\,6)$, $(0.8222,0.126\,102\,6)$, $(0.825,0.126\,102\,6)$, $(0.827,0.126\,102\,6)$, $(0.831,0.126\,102\,6)$, $(0.838,0.126\,102\,6)$. The first 4×10^5 iterations from the initial values were ignored, and then the following 1000 iterations were recorded to obtain the figure.

One of the period-2 elliptic points collides with the $\{(x,y)|x=x_{F_2}\}$ borderline at $b\simeq1.217\,74$ and then vanishes together with the elliptic island. Therefore in the parameter range $b\in(1.0,1.217\,74)$ a chaotic sea occupies the whole phase plane. It may be interesting that in parameter region $1.217\,74<b<1.324$ there is an almost forbidden region and a region with high visiting probability around the remaining elliptic island, as shown in Fig. 11. The almost forbidden region is apparently due to both the quasigap and the dissolving of some KAM cycles via the collision with the border. The iterations along these cycles will soon reach the protection region and then move along the chaotic orbits shown by dotted patterns. We have numerically certified that the region of high visiting probability situates along the homoclinic stable and unstable manifolds of a hyperbolic orbit. When $b<1$, the new elliptic point addressed by e_2 in the last section and one of the period-4 elliptic points fall in region F, so that e_1 remains the only elliptic point.

The whole bifurcation diagram is shown in Fig. 12. As can be seen the period-doubling bifurcation cascade is normal before line 2, that is, at $b\simeq1.37$. Between lines 2 and 3 more and more KAM cycles vanish via collisions with the border and become parts of the QT. All the QTs become stable chaotic orbits at line 3 (at $b\simeq1.324$) due to the vanishing of the leaking hole, but there is still a remaining part of the period-2 elliptic island. The main period-doubling bifurcation cascade is interrupted by a border-collision bifur-

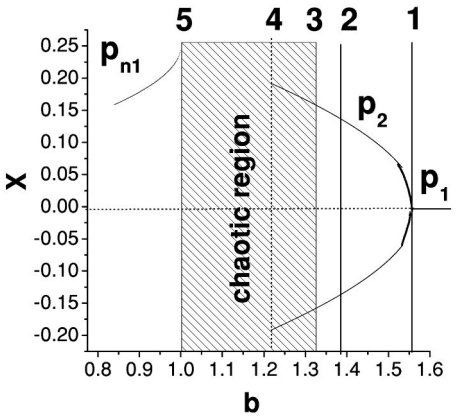

FIG. 12. The bifurcation diagram. Line 1 is at $b=\pi/2$. Line 2 is at $b=1.37$. Line 3 is at $b=1.324$. Line 4 is at $b=1.217\,74$. Line 5 is at $b=1$. Curve P_1 denotes the fixed point $(0.0,-a/b)$. Curve P_2 denotes the period-2 orbit produced after its first period-doubling bifurcation. Curve P_{n_1} denotes the elliptic point e_1 at $(\arcsin b/2\pi,-a/b)$. Other things are explained in the text.

cation at line 4 (located in $b\simeq 1.217\,74$), so that the system enters a complete chaotic sea. After line 5, a new elliptic point e_1 appears. It should be noted that the parameter range of the coexisting period-6 orbit crossing the border is too small to be shown in this bifurcation diagram.

V. DISCUSSION

We have discovered some ''quasidissipative properties'' in a system that is a concatenation of two area-preserving maps. These properties make the system behave partly dissipative and partly conservative. What is the physical or practical meaning of this discovery? In this circuit system it means that with the jumping changes induced by overvoltage protection some chaotic motion transfers to regular (periodic or quasiperiodic) motion, and that some regular motion can be changed to chaotic, as the special period-doubling bifurcation shows. Also, some phase regions may become prohibited or protected for iterations. These conclusions may be trivial.

However, we argue that in some types of concatenation systems this discovery may have much more interesting implications. For example, if some quantum systems can show the quasidissipative properties, their natures will be very interesting to research.

ACKNOWLEDGMENTS

This study was supported in part by grants from the Hong Kong Research Council (RGC) and the Hong Kong Baptist University Faculty Research Grant (FRG). It was also supported by the National Natural Science Foundation of China under Grant No. 19975039, the Foundation of Jiangsu Provincial Education Committee under Grant No. 98kjb14006, and China State Key Projects of Basic Research under the Grant No. G1999064509. The authors want to thank Professor Yan Gu for very important discussions and suggestions.

APPENDIX

As stated in Ref. [9], the differential equations describing variation of V are

$$\frac{dV_u}{dt}=\frac{E-V_u}{R_1C}, \tag{A1}$$

$$\frac{dV_d}{dt}=\frac{RE-R_1V_d}{R_1RC},$$

where R_1 or R_2 is charging or discharging resistance, respectively. E is the output voltage of a dc source. R satisfies $1/R=1/R_1+1/R_2$. After integrating the falling branch from t_n to t^*, and the rising branch from t^* to t_{n+1} in equation (A1), one has

$$RC\ln\frac{RE-R_1V_n}{RE-R_1V^*}=t^*-t_n, \tag{A2}$$

$$R_1C\ln\frac{E-V_{n+1}}{E-V^*}=t^*-t_{n+1}.$$

Let $V^*=U_{min}$, $x=\omega t$, and notice that $V_{n+1}=U_{max}-U_0\sin(\omega t_{n+1})$ and $V_n=U_{max}-U_0\sin(\omega t_n)$, one has

$$x_{n+1}+R_1C\omega\ln\frac{E-U_{max}+U_0\sin x_{n+1}}{E-U_{min}}$$

$$=x_n+RC\omega\ln\frac{RE-R_1U_{max}+R_1U_0\sin x_n}{RE-R_1U_{min}}. \tag{A3}$$

In Eq. (A3) let $A_1=\omega RC/2\pi$, $B_1=(R/R_1)E-U_{min}$, $C_1=(R/R_1)E-U_{max}$, $A_2=\omega R_1C/2\pi$, $B_2=(\omega R_1C/2\pi)\ln(E-U_{min})$, $C_2=E-U_{max}$; mapping (1) can be obtained.

[1] L. Glass, Chaos **1**, 13 (1991).
[2] P. Alstrøm and M. T. Levinsen, Phys. Lett. A **128**, 187 (1988).
[3] A. V. Holden and Y. Fan, Chaos, Solitons Fractals **2**, 349 (1992).
[4] H. Lamba and C. Budd, Phys. Rev. E **50**, 84 (1994).
[5] D.-R. He, E. J. Ding, M. Bauer, S. Habip, U. Krueger, W. Martienssen, and B. Christiansen, Europhys. Lett. **26**, 165 (1994).
[6] S. Guan, B.-H. Wang, D.-k. Wang, and D.-R. He, Phys. Rev. E **52**, 453 (1995).
[7] S.-X. Qu, B. Christiansen, and D.-R. He, Phys. Lett. A **201**, 413 (1995).
[8] S.-X. Qu, S. Wu, and D.-R. He, Phys. Rev. E **57**, 402 (1998).
[9] D.-R. He, B.-H. Wang, M. Bauer, S. Habip, U. Krueger, W. Martienssen, and B. Christiansen, Physica D **79**, 335 (1994).
[10] D.-R. He, M. Bauer, S. Habip, U. Krueger, W. Martienssen, B. Christiansen, and B.-H. Wang, Phys. Lett. A **171**, 61 (1992).
[11] C. Marriot and C. Delisle, Physica D **36**, 198 (1989).

[12] I. Dana, N. W. Murray, and I. C. Percival, Phys. Rev. Lett. **62**, 233 (1989).
[13] F. Borgonovi, G. Casati, and B. Li, Phys. Rev. Lett. **77**, 4744 (1996).
[14] F. Borgonovi, Phys. Rev. Lett. **80**, 4653 (1998).
[15] F. Borgonovi, P. Conti, D. Rebuzzi, B. Hu, and B. Li, Physica D **131**, 317 (1999).
[16] B. Hu, B. Li, J. Liu, and Y. Gu, Phys. Rev. Lett. **82**, 4224 (1999).
[17] H. E. Nusse, E. Ott, and J. A. Yorke, Phys. Rev. E **49**, 1073 (1994); H. E. Nusse and J. A. Yorke, Physica D **57**, 39 (1992).
[18] W. Zeng, L. Glass, and A. Shrier, Circ. Res. **69**, 1022 (1991).
[19] B. V. Chirikov, Phys. Rep. **52**, 265 (1979).
[20] S. J. Shenker and L. P. Kadanoff, J. Stat. Phys. **27**, 631 (1982).
[21] J. Wang, X. L. Ding, B. H. Wang, and D.-R. He, Chin. Phys. Lett. **18**, 13 (2001).
[22] O. B. Christensen and T. Bohr, Phys. Scr. **38**, 641 (1988).